Tellus
SERIES B
CHEMICAL
AND PHYSICAL
METEOROLOGY
PUBLISHED BY THE INTERNATIONAL METEOROLOGICAL INSTITUTE IN STOCKHOLM

Tellus (2010), 62B, 521–532

Printed in Singapore. All rights reserved

© 2010 CSIRO
Tellus B © 2010 International Meteorological Institute in Stockholm

TELLUS

Assessing the impact of crops on regional CO_2 fluxes and atmospheric concentrations

By K. D. CORBIN[1]*, A. S. DENNING[2], E. Y. LOKUPITIYA[2], A. E. SCHUH[2], N. L. MILES[3], K. J. DAVIS[3], S. RICHARDSON[3] and I. T. BAKER[2], [1]*Commonwealth Scientific and Industrial Research Organization (CSIRO), Marine and Atmospheric Research, Aspendale, Victoria, Australia;* [2]*Department of Atmospheric Science, Colorado State University, Fort Collins, CO, USA;* [3]*Department of Meteorology, Pennsylvania State University, University Park, PA, USA*

(Manuscript received 22 December 2009; in final form 30 June 2010)

ABSTRACT

Human conversion of natural ecosystems to croplands modifies not only the exchange of water and energy between the surface and the atmosphere, but also carbon fluxes. To investigate the impacts of crops on carbon fluxes and resulting atmospheric CO_2 concentrations in the mid-continent region of the United States, we coupled a crop-specific phenology and physiology scheme for corn, soybean and wheat to the coupled ecosystem–atmosphere model SiB3–RAMS. Using SiBcrop–RAMS improved carbon fluxes at the local scale and had regional impacts, decreasing the spring uptake and increasing the summer uptake over the mid-continent. The altered fluxes changed the mid-continent atmospheric CO_2 concentration field at 120 m compared to simulations without crops: concentrations increased in May and decreased >20 ppm during July and August, summer diurnal cycle amplitudes increased, synoptic variability correlations improved and the gradient across the mid-continent region increased. These effects combined to reduce the squared differences between the model and high-precision tower CO_2 concentrations by 20%. Synoptic transport of the large-scale N–S gradient caused significant day-to-day variability in concentration differences measured between the towers. This simulation study shows that carbon exchange between crops and the atmosphere significantly impacts regional CO_2 fluxes and concentrations.

1. Introduction

The conversion of natural ecosystems to croplands is one of the most direct manifestations of human activity within the biosphere (Ramankutty and Foley, 1998). Land use and land cover change affect the phenology of the vegetation, modify biophysical properties of the land surface (e.g. surface roughness and albedo) and alter biogeochemical cycles (Betts, 2005). Modelling studies have shown that these perturbations change the weather and climate on regional and global scales (Copeland et al., 1996; Bonan, 1997; Lawrence and Slingo, 2004; Osborne et al., 2007).

Although the conversion of forests and grasslands to agricultural land initially leads to a net release of carbon to the atmosphere (Houghton, 2003), the role of croplands on the carbon cycle remains uncertain. Studies over Europe suggest that on annual time-scales croplands are net carbon sources due to soil carbon loss, although these estimates are sensitive to land history, soil properties and management practices (Vleeshouwers and Verhagen, 2002; Janssens et al., 2003). On the global scale, Bondeau et al. (2007) found that including crops reduces the carbon sink in the land biosphere, as compared with simulations of the potential natural vegetation only.

To investigate regional carbon fluxes over a densely cultivated region, the North American Carbon Program (NACP) launched the Mid-Continent Intensive (MCI) Campaign (Ogle et al., 2006). The MCI region is centred over the Midwestern United States (Fig. 1), and the primary focus of the campaign is to compare and reconcile regional fluxes on hourly to annual time scales from top-down atmospheric budgets with bottom-up ecosystem model-based inventories. The MCI campaign funded dense inventory and flux measurements throughout the summer and fall of 2007. The region hosts networks of eddy-covariance flux towers, several long-term agricultural experimental sites with time series of carbon stocks, forestry data collected through the U.S. Department of Agriculture (USDA) Forest and Inventory Analysis (FIA) program, annual crop yield data collected by the USDA National Agricultural Statistics Service (NASS) and fossil fuel emissions estimates from the Environmental Protection Agency (EPA) Fuel Emission Statistics. In addition to local

*Corresponding author.
e-mail: katherine.corbin@csiro.au
DOI: 10.1111/j.1600-0889.2010.00485.x

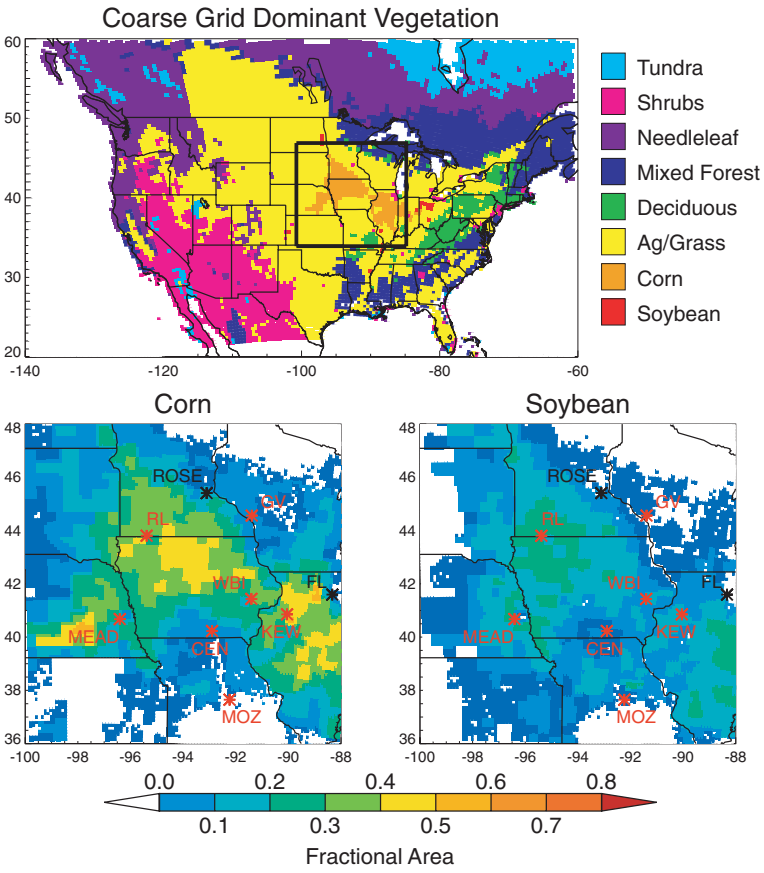

Fig. 1. Grid setup for the SiB3–RAMS simulations. (Top panel) The coarse domain and the dominant vegetation type. The interior grid, corresponding to the MCI region, is outlined on the coarse domain. (Bottom left panel) The fractional coverage of corn in the nested grid. Red tower labels indicate the continuous atmospheric CO_2 sites, and black tower labels indicate AmeriFlux sites. (Bottom right panel) The fractional coverage of soybean in the nested grid.

flux measurements and crop yields, high-precision atmospheric CO_2 concentrations are sampled at seven communications towers throughout the region, beginning spring 2007 (Richardson et al., 2009).

The dense network of data from the MCI can be used for a variety of studies, not only to investigate carbon fluxes between the land and atmosphere, but also to enhance our knowledge of the carbon cycle. Regional models provide a way to quantitatively map sources and sinks of CO_2 using a variety of different observations (i.e. soil maps, vegetation maps, topography, meteorology). Model simulations compared with field measurements from the MCI campaign will lead to the advancement of our understanding of the processes and mechanisms driving the variability in these fields. In addition to providing atmospheric inversions with initial flux estimates that include all known mechanisms, coupled ecosystem–atmosphere models can help interpret the high-frequency variability in atmospheric CO_2 concentrations. Because CO_2 concentrations contain information about all sources and sinks of carbon, understanding the mechanisms driving the CO_2 variability will help us better predict carbon fluxes.

To evaluate and analyse atmospheric CO_2 concentrations, it is essential that carbon fluxes be modelled as accurately as possible using all available information. Due to physiological and phenological differences from natural ecosystems, crops strongly modify both the seasonality and magnitude of carbon fluxes by having shorter growing seasons with more intense drawdown (de Noblet et al., 2004; Gervois et al., 2004; Lokupitiya et al., 2009); and land surface models typically do not represent crop fluxes well due to their short but vigorous photosynthetic uptake. Traditionally, models use remotely sensed vegetation parameters, such as the normalized difference vegetation index (NDVI), leaf-area index (LAI) and the fraction of photosynthetically active radiation (FPAR) to estimate carbon dynamics; however, using satellite data does not accurately capture planting, growth, and harvest events of crops due to temporal and spatial compositing. Remotely sensed products use temporal composites, generally 8-day to monthly, to minimize cloud contamination. Because the LAI and FPAR for crops rapidly changes, using these coarse time resolutions do not accurately capture the magnitude of the crop growth and unrealistically extend the timing of the growing season. Spatial compositing also occurs and leads to misrepresentations between the data and the actual field conditions.

To better predict carbon exchanges for crops, Lokupitiya et al. (2009) developed crop-specific phenology and physiology sub-models for corn (maize), soybean and wheat and coupled them to the Simple Biosphere Model (SiBcrop). The sub-models replace the remotely sensed LAI and FPAR used in SiB for estimating

carbon dynamics. Using a phonologically based model substantially improved the prediction of LAI for crops, and the use of crop-specific physiology increased the carbon fluxes for a specified LAI to better predict the net ecosystem exchange (NEE) as compared with observed data at flux tower sites in the U.S. mid-continent region (Lokupitiya et al., 2009).

To predict regional-scale carbon exchanges and the resulting atmospheric CO_2 concentrations, we coupled the corn, soybean and wheat sub-models to the ecosystem–atmosphere model SiB3–RAMS. In this study, we will investigate the impact of crops on atmospheric CO_2 concentrations. To evaluate simulated carbon fluxes, we will compare modelled NEE to eddy-covariance derived NEE from flux towers. We will also evaluate atmospheric CO_2 concentrations by comparing the modelled CO_2 field to continuous concentrations sampled on towers at 30 and 120 m during the MCI campaign. In addition, we will examine the cause of the variability in the CO_2 gradient between the towers.

2. Methods

2.1. Model: SiB3–RAMS

The base model used in this study is the Simple Biosphere Model Version 3 (SiB3; Baker and Denning, 2008) coupled to the Brazilian version of the Colorado State Regional Atmospheric Modelling System (RAMS; Frietas et al., 2005). The coupled model, SiB3–RAMS, has been evaluated and used in a variety of carbon studies. Denning et al. (2003) used the coupled model to investigate the influence of ecosystem fluxes on atmospheric CO_2 concentrations in Wisconsin; and in a companion paper, Nicholls et al. (2004) showed that katabatic winds, vertical wind shear and circulations in the vicinity of lakes caused atmospheric CO_2 variations. Lu et al. (2005) used the model to investigate mesoscale circulations and atmospheric CO_2 variability in South America. Wang et al. (2007) investigated synoptic variability in atmospheric CO_2 concentrations over North America; and Corbin et al. (2008) used SiB–RAMS to evaluate atmospheric CO_2 spatial and temporal variability. Throughout these studies, various SiB–RAMS modelled fields have been evaluated against observations, including temperature, wind speed, wind direction, precipitation, radiation, water vapour mixing ratio, latent heat, sensible heat, NEE and atmospheric CO_2 concentrations. Because this is a model comparison study to investigate the impact of crops on carbon fluxes and atmospheric concentrations, we focus on NEE and atmospheric CO_2 concentrations, referring the reader to these previous studies for further model evaluation.

Traditionally, SiB used remotely sensed NDVI to calculate LAI and FPAR; however, due to both spatial and temporal compositing, these satellite data do not accurately capture the timing of planting and harvest events and underestimate the maximum LAI and FPAR values for crops. To more accurately simulate croplands, we coupled SiB3–RAMS to the crop module developed by Lokupitiya et al. (2009). The crop module explicitly calculates the LAI and FPAR for corn, soy and wheat. These simulated values replace remotely sensed data for these vegetation classifications. Phenology events and growth stages for crops were determined by the growing degree days and the number of days since planting, and the crop module allocated photosynthetic carbon to four different plant pools depending on phenological development. The daily carbon allocation to leaves was used to update LAI, which was then used to calculate the NEE.

SiB3–RAMS utilizes a variety of data sets. All the data are for 2007 and are re-gridded from their native resolutions to the SiB3–RAMS domain. The land cover classification is derived from the Moderate Resolution Imaging Spectroradiometer (MODIS) data with 1 km horizontal resolution, which is distributed by the Land Processes Distributed Active Archive Center (LP DAAC) located at the U.S. Geological Survey (USGS) Earth Resources Observation and Science (EROS) Center (lpdaac.usgs.gov). The land cover is converted from the University of Maryland (UMD) classification scheme to SiB biome types. Corn, soybean and wheat are integrated into the vegetation map based on county-level ground-based data from the National Agricultural Statistics Service (NASS) and the Census of Agriculture (AgCensus) (Lokupitiya et al., 2007).

Rather than calculating LAI and FPAR from remotely sensed NDVI, SiB3–RAMS uses direct estimates of these parameters from satellite data. Both LAI and FPAR are 8-day composites derived from MODIS 1-km resolution data, and these products are provided by the Numerical Terradynamics Simulation Group at the University of Montana (Zhao et al., 2005). Due to the minimal land cover classification information provided with the data, the 1-km resolution data are combined to provide one estimate of LAI and FPAR per grid cell. For grid cells that include crops, the LAI and FPAR values for corn, soybean and wheat are replaced by calculated values from the crop module.

The soil classification is derived from a 5-min resolution soil type map by the International Geosphere Biosphere Programme (IGBP) (IGBP, 2000). Meteorological fields are initialized and nudged to the National Centers for Environmental Prediction (NCEP) North American Regional Reanalysis (NARR) meteorological analyses, which covers the North American domain with a 32-km horizontal resolution, 3-h temporal resolution and 50-hPa vertical resolution (Mesinger et al., 2006). The NCEP NARR data are provided by the NOAA/OAR/ESRL Physical Sciences Division located in Boulder, CO, USA, from their web site at http://www.esrl.noaa.gov/psd/. Fossil fuel emissions are prescribed from the high-resolution Vulcan fossil fuel inventory (Gurney et al., 2009). Since the Vulcan emissions represent 2002, they are scaled to match the total estimated 2007 emissions from the Energy Information Administration (EIA, 2007), and these fluxes are added to the first model level. Initial values for carbon pools, soil moisture and other prognostic variables are calculated

for every grid cell from a 10-yr offline SiBcrop simulation using NARR driver data from 1997 to 2007. The initial atmospheric CO_2 concentration field and the lateral boundary concentrations are set and nudged to 3-hourly global CO_2 concentrations on a $1.25^\circ \times 1^\circ$ grid from the Parameterized Chemical Transport Model (PCTM; Parazoo et al., 2008).

2.2. Case descriptions

Three SiB3–RAMS simulations over North America are performed for 1 May 2007 through 31 August 2007. The coarse grid for all cases has 200 × 120 grid points with 40-km horizontal grid increments, 46 vertical levels up to 24 km and a 90 s time-step. To capture subgrid-scale variability in land cover, SiB3–RAMS uses three vegetation patches per grid cell. The dominant vegetation cover for the coarse grid is shown in Fig. 1 (top panel). The landcover in the MCI region is dominated by corn, soybean and C3 grasses/agriculture.

The first case, which will be referred to as BASE, uses the original SiB3–RAMS (without the crop module) and resets all the corn, soybean and wheat biomes to the generic agriculture/grassland vegetation type. The second case, CROP, uses the crop phenology module to replace the remotely sensed LAI and FPAR for corn, soybean and wheat. The crop module also uses crop-specific physiology to replace the generic grassland/agricultural parameters. The third case, CROPN, uses the crop module and includes a nested grid over the MCI region to capture the extensive corn and soybean cover (Fig. 1, bottom panel). The horizontal grid spacing for the interior grid is 10 km.

2.3. Observations

Because SiB3–RAMS calculates both carbon fluxes and concentrations, we will evaluate the model performance using measurements of both eddy-covariance derived NEE and CO_2 concentrations. For carbon fluxes, eddy-covariance derived NEE data for 2007 are available at three AmeriFlux towers in the mid-continent region: the Mead Rainfed site in Nebraska (MEAD; 41.12°N, 96.44°W; Verma et al., 2005), the Rosemount G21 conventional management corn/soybean rotation site in Minnesota (ROSE; 44.71°N, 93.09°W; Griffis et al., 2008) and the Fermi Agricultural conventional tillage corn/soybean rotation site in Illinois (FL; 41.86°N, 88.22°W; Matamala et al., 2008; Xiao et al., 2008). At all towers, the NEE estimates are derived from measurements of carbon flux and storage, and we use the gap-filled data products. Corn grew at the Mead and Rosemount sites during the summer of 2007, while soybean grew at the Fermi site. The data were obtained from FLUXNET and are available on-line at http://www.fluxnet.ornl.gov (Baldocchi, 2001).

To compare these flux measurements to SiB3–RAMS fluxes, we sample the model at the grid-cell including the tower. Because SiB3–RAMS has three patches per grid cell, only the patch with the corresponding vegetation type is used for comparison (i.e. grass/agriculture for BASE and either corn or soy for CROP). For the CROP and CROPN cases, the fluxes at the towers are nearly identical despite the difference in horizontal resolution, and we only present the results from the CROPN case.

To evaluate modelled CO_2 concentrations, we compare simulated concentrations to continuous tower measurements. As part of the MCI campaign, Pennsylvania State University (PSU) collected continuous atmospheric CO_2 concentrations on five communications towers and in the mid-continent region (Richardson et al., 2009). These measurements were sampled using cavity ring-down spectroscopy instruments from Picarro (Crosson, 2008). In addition, PSU sampled continuous, well-calibrated CO_2 concentrations on the AmeriFlux tower at Missouri Ozarks, which is located in the transitional zone between the central hardwood region and the central agricultural region of the U.S. Atmospheric CO_2 concentrations for 2007 were also collected at West Branch, Iowa (WBI) by the National Oceanic and Atmospheric Administration (NOAA) Global Monitoring Division (GMD). High-accuracy CO_2 concentrations were sampled at WBI using a non-dispersive infrared spectroscopy CO_2 analyser, and the data are publicly available at http://esrl.noaa.gov/gmd (Andrews et al., 2009). The reference names and letters, locations and sampling heights at all six towers are displayed in Table 1 and Fig. 1, bottom panel. Nearly all the towers measure CO_2 concentrations both near the surface and in the mid-troposphere, except the Missouri Ozark tower, which only collects samples at 30 m. We will compare measurements sampled closest to 30-and 120 m at each tower to model results from the matching location at the same vertical level. To reconcile an offset, the four-month mean modelled atmospheric CO_2 concentrations were corrected to match the four-month mean observed CO_2 concentration among the towers.

3. Results

3.1. Crop impacts on NEE

Simulating corn and soybean explicitly using crop-specific physiology and phenology rather than using the generic agriculture/grassland biome significantly alters both the timing and the magnitude of NEE (Fig. 2). In the BASE case, the NEE is similar at all three sites, with a diurnal mean NEE of $\sim -3\ \mu\text{mol m}^{-2}\ \text{s}^{-1}$ throughout the summer. The NEE remains relatively constant due to the remotely sensed LAI and FPAR for this time period, as the satellite data has reduced seasonality due to both temporal and spatial compositing. In addition, re-gridding the data to the SiB3–RAMS domain causes further smoothing. Because the remotely sensed vegetation data associated with the LAI and FPAR has limited land cover classifications and does not contain crops, all the satellite pixels within a SiB3–RAMS grid cell are included to create a mean value. Because crops have a much shorter, more intense growing season than natural vegetation,

Table 1. Reference name, location and sampling height for the towers measuring continuous atmospheric CO_2 concentrations in the MCI region

Reference	Abbreviation	Site	Latitude	Longitude	Sampling heights
A	MEAD	Mead, NE	41.14°N	96.46°W	30/122 m
B	RL	Round Lake, MN	43.53°N	95.41°W	30/110 m
C	CEN	Centerville, IA	40.79°N	92.88°W	30/110 m
D	WBI	West Branch, IA	41.73°N	91.35°W	31/99/379 m
E	GV	Galesville, WI	44.09°N	91.34°W	30/122 m
F	KEW	Kewanee, IL	41.28°N	89.97°W	30/140 m
G	MOZ	Missouri Ozark, MO	38.74°N	92.20°W	30 m

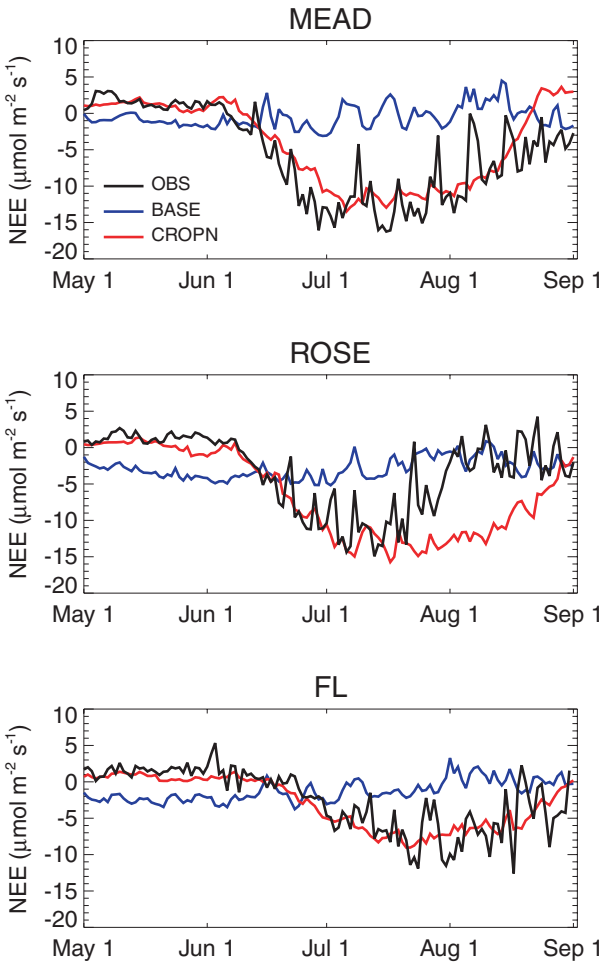

Fig. 2. Diurnal mean net ecosystem exchange (NEE) at the Mead site (top panel), the Rosemount G21 site (middle panel) and the Fermi site (bottom panel). Observations are solid black, modelled NEE from the BASE simulation is dark grey solid dot, and modelled NEE from the CROPN simulation is dashed grey.

averaging over all satellite pixels further lengthens the growing season and reduces the amplitude of the seasonality in LAI and FPAR. These temporal and spatial compositing effects combine to yield relatively constant NEE from May to August.

In the simulations with crops, the NEE varies between sites and more closely matches the observations. Over the two corn sites (MEAD and ROSE), the NEE remains small until the beginning of June when the corn begins to grow rapidly. The NEE uptake rapidly increases through June, reaching maximum daily carbon uptake throughout July in both the eddy-covariance derived NEE estimates and the simulations by the crop model. The uptake then decreases throughout August; however, at the Rosemount site the carbon uptake in the model does not decrease as rapidly as seen in the observations.

Compared with corn, soybean starts to grow later in the year and assimilates less carbon (FL; Fig. 2, bottom panel). At the soybean site, the crop module captures the minimal drawdown from May until mid-June, the rapid increase in uptake throughout late June and July, and the decrease in uptake in late August. Modelling corn and soy explicitly yields a shorter, more intense growing season than using natural ecosystems to represent crops, which better represents the eddy-covariance derived fluxes at both corn and soybean sites.

Atmospheric CO_2 concentrations are influenced not only by local carbon fluxes, but also by more distant fluxes through atmospheric mixing and transport. Because the MCI region is located in the middle of the United States, it is important to understand the fluxes over the entire country. The mean spring (May) and summer (JJA) NEE from the CROP simulation are displayed in Fig. 3 (left panel). In May of 2007, the majority of the country is taking up carbon at the onset of the growing season, except heavily cultivated areas including the MCI region. Since corn and soybean have not started growing, the central United States is neutral to a slight source of carbon due to bare fields at these locations. During the summer of 2007, the model shows that the southeastern United States is a source of CO_2. Photosynthesis is severely reduced due primarily to temperature and humidity stress. During the daytime, high temperatures significantly above optimal conditions decrease the assimilation while enhancing the respiration, and the dry atmospheric conditions create a vapour pressure deficit which further restricts carbon uptake. According to the National Climatic Data Center, the summer of 2007 was the sixth warmest for the United States in the past 113 yr, with temperatures being the highest in the

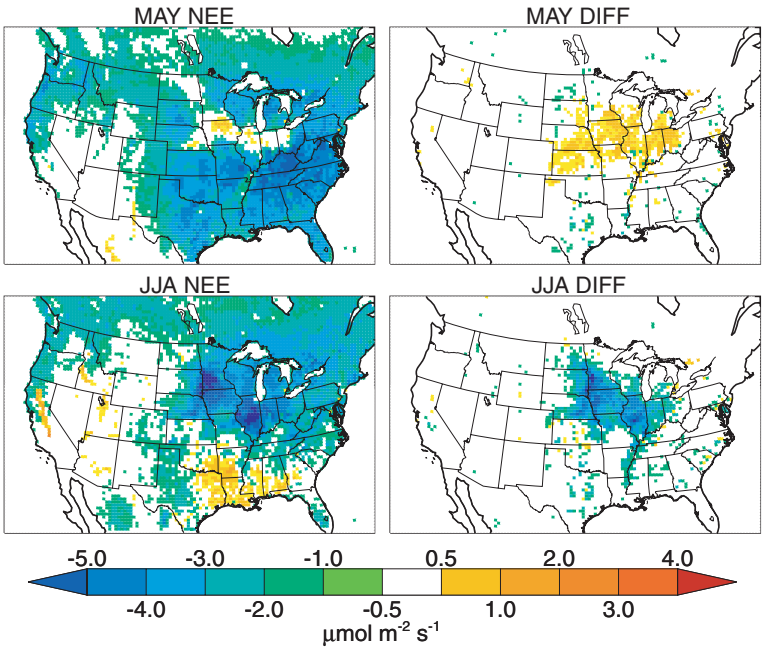

Fig. 3. (Top left panel) Mean May NEE from the CROPN simulation. (Bottom left panel) Mean summertime (June/July/August) NEE from the CROPN simulation. (Top right panel) Mean May NEE differences between the BASE and CROPN simulations (CROPN–BASE). (Bottom right panel) Mean summertime NEE differences.

southeast and in the west. The southeastern United States experienced a heat wave in August, breaking over 70 records for all-time high temperatures and for the most days above 32 °C, and the 3-month Standardized Precipitation Index for June through August 2007 shows that the southeastern United States was exceptionally dry (National Oceanic and Atmospheric Administration National Climatic Data Center; http://lwf.ncdc.noaa.gov/climate-monitoring/index.php). Central California was also very hot and moderately dry according to the Climatic Data Center, and this region is also a summer source of CO_2 due to temperature and humidity stress. The northern half of the United States and Canada are summer sinks of carbon. The MCI region is a particularly large summer sink, with some heavily cultivated regions taking up more than 8 μmol m^{-2} s^{-1} carbon on average.

Simulating crops alters the modelled NEE across the entire MCI region (Fig. 3, right panel). In May, the CROPN case has reduced monthly mean uptake over the MCI and Midwest regions compared to the BASE simulation, with mean differences of ∼1–3 μmol m^{-2} s^{-1}. These differences are caused by the lack of uptake in corn and soybean during this month while the crops are sown as compared with the BASE case, which has photosynthesizing natural vegetation. A few individual grid cells have enhanced uptake over the central United States, and these pixels correspond to wheat crops that are nearing maturity after being planted in the winter. The mean May fluxes over the MCI region do not change between the CROP and CROPN simulations.

In the summer, modelling crops explicitly enhances the uptake over the MCI region, with differences greater than 5 μmol m^{-2} s^{-1} in the seasonal average. The enhanced summer uptake from including crops is due to the intensity of assimilation by both corn and soybean compared with the basic agricultural and natural grassland fluxes. Simulating corn and soybean rather than generic agriculture has the largest impact on the NEE, as the majority of the summer difference is seen between the CROP and BASE cases. Adding the nested grid contributes an additional ∼1–2 μmol m^{-2} s^{-1} to the mean summer sink.

3.2. *Crop impacts on atmospheric CO_2 concentrations*

Mean atmospheric CO_2 concentrations at 120 m in the CROPN simulation reflect the 2007 NEE distribution (Fig. 4, left panels). In May, concentrations are lower in the southeast, central United States, and eastern Canada compared to higher concentrations in the west and the MCI region. In contrast, summer (JJA) concentrations are high over the southeast, where the region is a source of carbon, whereas lower concentrations exist over the northern United States and Canada, where the vegetation is a sink. High concentrations appear over southern California and the east coast from fossil fuel emissions. The high southern and eastern concentrations and low northern concentrations create a large-scale horizontal gradient in atmospheric CO_2 concentrations, with near-surface differences at 120 m greater than 20 ppm across the central states just to the south of the MCI region.

Including crops causes significant, spatially coherent changes in the 120 m atmospheric CO_2 concentrations (Fig. 4, right panels). The CROPN simulation has higher concentrations over the MCI region in May compared to the BASE case. The increased concentrations occur due to the lack of uptake over croplands before planting. The May differences between the CROP and CROPN simulations are minimal (<1 ppm, not shown). In the

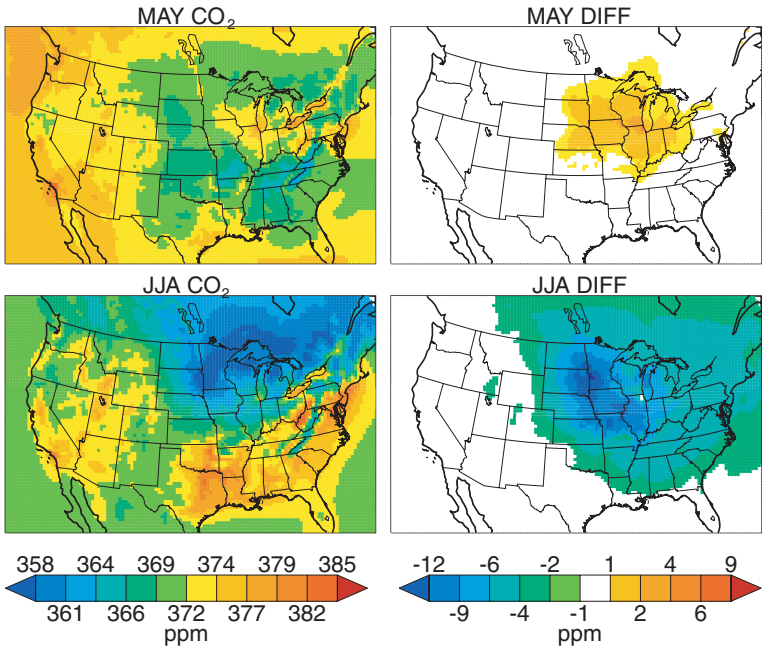

Fig. 4. (Top left panel) Mean May atmospheric CO_2 concentrations at 120 m from the CROPN simulation. (Bottom left panel) Mean summer (JJA) atmospheric CO_2 concentrations at 120 m from the CROPN simulation. (Top right panel) Mean May 120 m CO_2 concentration differences between BASE and CROPN (CROPN–BASE). (Bottom panel) Mean summer (JJA) 120 m CO_2 concentration differences.

summer, the CROPN simulation has significantly lower concentrations than the BASE case. Maximum differences occur in July, when 120 m concentration differences are greater than 15 ppm. Approximately half of the net differences seen between the CROPN and BASE cases are due to adding crops on the coarse domain, the other half are due to including the nested grid over the MCI region. Throughout the summer, the influence of crops extends to Canada due to atmospheric transport, although the magnitude of the differences decreases with increasing distance from the MCI region.

The impact of crops on atmospheric CO_2 concentrations can be quantitatively assessed by evaluating the concentrations at the seven towers in the MCI region. The root mean square errors (RMSE) between the full time-series of tower observations and the SiB3-RAMS simulations are shown in Table 2. At 120 m, including the crop module lowered the RMSE at all towers. Including crops on the coarse domain caused the largest reduction, while increasing the spatial resolution to capture the extensive crop coverage further reduced the errors. The RMSE reduction is more than 25% at Round Lake and Kewanee, the two towers with the greatest coverage of corn and soybean; however, the error reduction at the Galesville tower is minimal. Overall, the mean RMSE at 120 m for the CROPN simulation is approximately 20% lower (2.4 ppm) than that for the BASE case. Model errors near the surface (30 m) are higher than those at 120 m, and the improvements in the CROP and CROPN simulations are less significant, except at WBI where the improvement is larger near the surface. The mean RMSE for the CROPN simulation is approximately 13% lower (2.4 ppm) than the BASE simulation, although the errors at both Mead and Galesville increase

Table 2. Root mean square errors (RMSE), in ppm, using the complete time series

	RMSE at 120 m (ppm)				RMSE at 30 m (ppm)			
Site	BASE	CROP	CROPN	% Error reduction	BASE	CROP	CROPN	% Error reduction
MEAD	12.5	11.6	11.1	12%	14.5	15.7	15.5	−7%
RL	14.1	10.5	10.1	28%	16.4	13.7	13.2	20%
CEN	15.2	12.6	11.9	22%	16.2	15.0	14.2	13%
WBI	17.5	14.7	14.0	20%	26.0	27.9	18.5	29%
GV	13.0	12.7	12.7	3%	19.6	20.4	20.5	−5%
KEW	15.8	13.1	11.4	28%	17.5	17.3	13.8	21%
MOZ	–	–	–	–	20.3	19.0	17.8	14%

Note: The left-hand columns show the errors at 120 m, and the right-hand columns display the errors at 30 m. The errors for the BASE, CROP and CROPN simulations are shown at each tower for both vertical levels, as is the percent error reduction between the BASE and CROPN simulations.

slightly when crops are modelled. The net error reductions show that including crops substantially improves the SIB3-RAMS simulations, particularly at the locations in heavily cultivated areas.

The improvement in the atmospheric CO_2 concentrations is caused by changes in the spring and summer drawdown, the diurnal cycle, and synoptic variability. Focusing on the Kewanee tower, which has the largest percentage of crop coverage, mid-afternoon mean concentrations and a ten-day mid-July time-series from both the tower CO_2 observations and all three model simulations are shown in Fig. 5. The BASE case does not capture the seasonality of the concentrations, with lower than observed CO_2 concentrations in May and June (>10 ppm differences) and higher values in July and August (>15 ppm differences). Simulating crops more closely matches the spring and summer drawdown by increasing the May concentrations and decreasing the mid-summer concentrations. Coarsely simulating crops helps to capture the seasonality, while modelling the region at higher resolution leads to further improvement. Including crops improves the synoptic variability at Kewanee, as specific events are captured in both the CROP and CROPN cases. The diurnal cycle also matches the observations more closely in the runs with crops, as the BASE simulation tends to underestimate the amplitude of the diurnal cycle. Improved summer drawdown and diurnal and synoptic variability all combine to cause the reduction in RMSE seen at Kewanee. Although the RMSE from the full time-series remains relatively large, the reduction from crops is still substantial and will improve both forward and inverse models. In particular, not capturing the correct magnitudes of concentrations in May and July by inaccurately modelling the spring drawdown will lead to biases in forward modelling applications and thus cause biases in carbon fluxes from inverse modelling studies.

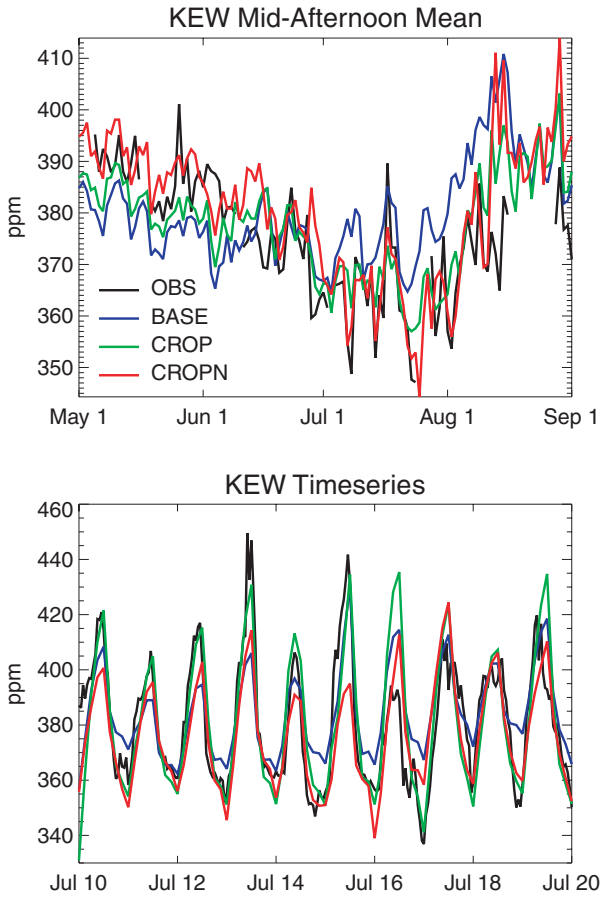

Fig. 5. (Top panel) Time-series of the mean mid-afternoon (12 p.m.–6 p.m.) atmospheric CO_2 concentrations at 120 m for the Kewanee tower, which is the tower with the greatest corn and soybean coverage. Observations are solid black, modelled CO_2 from the BASE simulation is dark grey solid dot, modelled CO_2 from the CROP simulation is grey dot and modelled CO_2 from the CROPN simulation is dashed grey. (Bottom panel) Mid-July 120 m time-series at the Kewanee tower.

In addition to Kewanee, all the towers in the MCI region show that modelling crops improves the spring draw-down, the diurnal cycle, and synoptic variability. Fig. 6(a) shows daytime monthly mean concentrations at each of the towers. The observations have high concentrations in May and low concentrations in July, with a spring drawdown of more than 20 ppm at some towers. The gradient between the towers increases throughout the growing season: in May, the towers are all within 5 ppm of each other, while in August the spread has increased to nearly 15 ppm. In July, three of the towers have daytime mean concentrations lower than 360 ppm.

The BASE simulation does a poor job capturing the drawdown during spring months, with mean concentrations remaining stable between May and July. The BASE case simulates an increase in the gradient between the towers located in cultivated areas; however, the model underestimates the May and June concentrations at the Missouri Ozark site. Including crops dramatically improves the simulated carbon uptake during the spring and summer. The CROP simulation increases the seasonality, and the CROPN case simulates even greater drawdown between spring and summer. The CROPN simulation still underestimates the May and June concentrations, particularly at Missouri Ozark. The CROPN case captures the increasing gradient between the towers and simulates the June and July spread reasonably well; however, it underestimates the monthly-mean May concentration at Missouri Ozark and overestimates the spread in August. In May, the highest concentrations amongst the agricultural towers occur at Round Lake, a densely cultivated region with minimal spring photosynthetic uptake, while the lowest concentrations occur at Centerville, located in a less-densely cropped region. In August, the lowest CO_2 concentrations occur at Round Lake and the highest concentrations occur at the Missouri Ozark site in both the observations and in the crop cases.

Monthly mean near-surface diurnal amplitudes at each tower are displayed in Fig. 6(b). The amplitude of the diurnal cycle increases throughout the growing season amongst the cropland

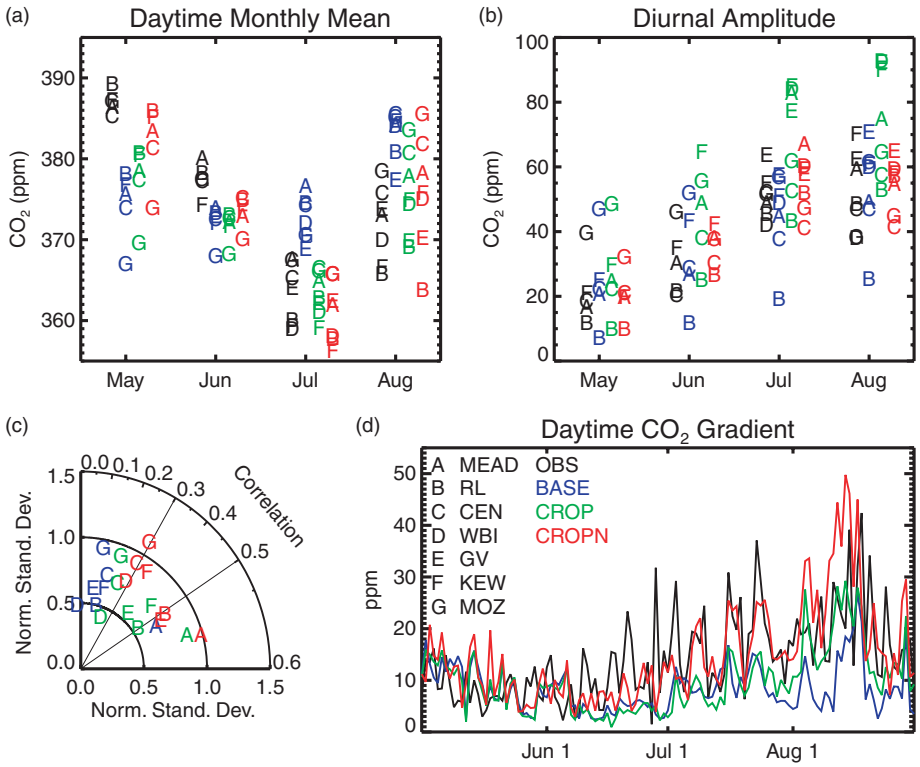

Fig. 6. (a) Mid-afternoon (12 p.m.–6 p.m.) monthly mean concentrations at 120 m (except MOZ, at 30 m) for each of the towers, which are indicated by individual letters. Observations are shown in black (left column), BASE results in blue (mid-left column), CROP results in green (mid-right column) and CROPN results in red (right column). (b) Monthly mean diurnal amplitudes at 30 m for each of the towers. (c) Taylor diagram of the mean mid-afternoon (12 p.m.–6 p.m.) atmospheric CO_2 concentrations at 120 m (except MOZ, at 30 m) for the BASE (blue), CROP (green) and CROPN (red) cases. A spline fit to the concentrations has been subtracted at every tower to remove seasonality to isolate synoptic variability. (d) Atmospheric CO_2 concentration gradient between the towers (obs, black; BASE, blue; CROP, green; CROPN, red). The gradient is the difference between the lowest and highest mid-afternoon 120 m (except MOZ, at 30 m) CO_2 concentration between the towers.

towers. In May, the diurnal amplitudes at the six heavily cultivated towers are less than 20 ppm, with a spread of 10 ppm. The minimal amplitudes are due to limited spring crop uptake, while the diurnal amplitude at the transitional site, Missouri Ozark, is considerably higher. In May, the BASE simulation overestimates the amplitude of the atmospheric CO_2 diurnal cycle at all the towers except Round Lake. The model simulates an increase in the amplitude of the diurnal cycle of CO_2 concentrations throughout the summer; however, it continues to underestimate the amplitude at Round Lake the entire summer. Including crops again generally matches the observations more closely, as both crop cases simulate smaller amplitudes over croplands in May that increase throughout the summer; however, the CROP case over-estimates the diurnal amplitudes in July and August. The CROPN case captures the magnitudes of the diurnal amplitude reasonably well, which is likely due not only to the inclusion of crops but also to the increased horizontal resolution in the simulation improving the boundary layer dynamics in the model.

To investigate synoptic variability, a Taylor diagram of daytime mean atmospheric CO_2 concentrations, with the springtime drawdown removed, is displayed in Fig. 6(c). Including the crop module increases the correlation at all the towers, indicating that the timing of the synoptic variability is better simulated when crops are modelled explicitly. Nesting over the MCI region further increases the correlations. Except at Missouri Ozark, the normalized standard deviations are all closer to unity in the CROPN simulation, indicating the magnitude of synoptic events has increased in the model and is closer to observed. At Missouri Ozark, the transitional site, the standard deviation is overestimated in the CROPN simulation. This is caused by a significant increase in concentrations during mid-August.

In addition to evaluating the atmospheric CO_2 concentrations at the individual towers, the magnitude of the gradient between towers can also be evaluated. Fig. 6(d) displays the time-series of the CO_2 gradient, which is the difference between the towers with the highest and lowest daytime mean concentrations. As indicated previously, the gradient increases from a mean magnitude of $\sim$10 ppm in May to mid-August, when the gradient is more than 20 ppm across the MCI region. Fig. 6(d) shows the gradient also has considerable day-to-day variability. The BASE simulation does not capture the increase in the gradient

and poorly simulates the timing and magnitude of the variability. By including crops, the CROP simulation captures the increase in the gradient during August. The CROPN simulation does a reasonable job at capturing both the magnitude as well as the timing of the day-to-day variations, particularly in July; however, this case overestimates the gradient the first half of August.

The cause of the day-to-day variability in the CO_2 differences amongst the towers can be investigated by analysing a time period in the CROPN case when both the model and the observations show a large change in the gradient. On 24 July the gradient across the towers is one of the largest seen during the summer, with a change of ~35 ppm across the MCI region. The CO_2 concentration map shows that the large-scale gradient is shifted northward by strong near-surface winds (Fig. 7, left panel). Zooming in to the MCI region shows that the gradient occurs through the centre of the towers. The Mead tower has higher concentrations (greater than 360 ppm), while the Kewanee tower has very low concentrations (less than 335 ppm) both from local crops as well as from the enhanced uptake over Illinois being advected northward. Two days later, on 26 July, the atmospheric CO_2 concentration difference between the towers is less than 10 ppm. Relatively low concentrations extend across the entire MCI region, as the low northerly concentrations are advected south due to a low pressure system cantered over the Great Lakes (Fig. 7, right panel). The large-scale gradient is shifted southward and lies completely below the MCI region, and all of the towers see lower concentrations that are within 10 ppm.

Although the atmospheric CO_2 concentrations are only displayed for two days, we investigated other cases when the CO_2 gradient jumped between high and low values and found similar results. High gradients occur when the mean wind is southerly, causing high concentrations from the south to be advected northward. This synoptic weather pattern causes the large-scale gradient to shift over the MCI region, thus causing large differences in the concentrations between the towers. On days when the gradient between the towers is low, the wind is from the north, advecting lower CO_2 further south and causing all the towers in the MCI region to have lower, relatively similar concentrations. The simulated gradient overestimation in August is due to very high concentrations seen at the Missouri Ozark and Mead towers, suggesting the model may be overestimating the stress in the southeast during the heat wave. The CROPN simulation shows that changes in the magnitude of the gradient are due to synoptic weather patterns shifting the location of the large-scale gradient between the high southeastern CO_2 concentrations and the low central and northern concentrations.

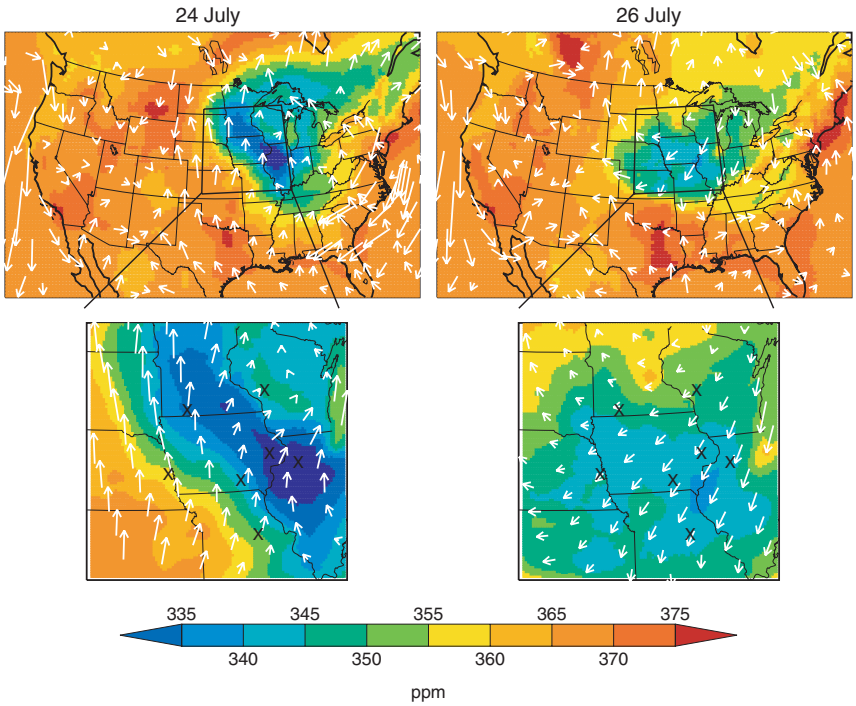

Fig. 7. (Left panel) Mean CROPN daytime atmospheric CO_2 concentrations at 120 m on 24 July 2007, with the corresponding mean wind vectors overlaid. The top panel shows the concentrations from the coarse domain, and the bottom panel shows the concentrations from the nested grid. The towers are indicated by the black Xs. (Right panel) Mean CROPN daytime atmospheric CO_2 concentrations at 120 m on 26 July 2007.

4. Conclusions

Simulating corn and soybean explicitly has a significant impact on both the timing and the magnitude of carbon fluxes. Compared to the generic agriculture land cover classification, the growing season for both corn and soybean is shortened and intensified, and crop-specific fluxes more closely match available observations. Since the mid-continent region of the U.S. is heavily cultivated, crops alter carbon fluxes on regional scales. In May, the monthly-mean carbon uptake over the central U.S. was reduced compared to natural vegetation, while the summer (JJA) carbon sink increased by more than 1.7 kg C m^{-2}.

Altering the carbon fluxes impacted the atmospheric CO_2 concentrations. Modelling corn and soybean enhanced the springtime drawdown, causing increased atmospheric CO_2 concentrations in May and significantly decreased concentrations during the summer, when daytime monthly-mean values less than 360 ppm occurred in both the model and in observations. These CO_2 concentration differences between modelling generic biomes and specific crop types were coherent over the mid-continent region in May and even extended to the eastern U.S. and Canada during the summer, causing changes greater than 15 ppm near the surface. Simulating crops explicitly increased the amplitude of the diurnal cycle in July and August and improved the timing and magnitude of CO_2 variability due to synoptic events. Compared with continuous CO_2 concentrations collected across the mid-continent region, the crop module significantly improved the concentrations, reducing the average RMSE at 120 m by 20%.

Including crops in the model captured the day-to-day variability in the mid-continent region and increased the atmospheric CO_2 concentration gradient across the mid-continent region, more closely matching the observed gradient in the central United States. Analysing the simulation with crops revealed that the considerable day-to-day variability in the gradient was due to synoptic variability. The summer of 2007 was exceptionally hot and dry over the southeastern United States, creating a summertime source of carbon in that region. This source increased the atmospheric CO_2 concentrations, and combined with fossil fuel emissions across the east coast, established a large-scale CO_2 gradient across the mid-continent. This large-scale near-surface gradient of over 30 ppm shifted with the weather patterns: southerly mean flow shifted the gradient northwards into the mid-continent causing high concentration differences between the towers, whereas northerly mean flow associated with low-pressure systems across northern United States and Canada shifted the large-scale gradient south and minimized the concentration differences seen across the mid-continent.

Crops significantly altered both carbon fluxes and atmospheric CO_2 concentrations on regional spatial scales and monthly time scales. Using natural vegetation to represent crops creates biases in forward models, and thus will create errors in source and sink estimates from atmospheric inverse models. Because crops are physiologically and phenologically different compared to forests and grasslands, it is essential to represent them in land surface models used for carbon studies, as these differences dramatically changed the regional carbon source and sink estimates, as well as regional atmospheric CO_2 concentrations.

5. Acknowledgments

The authors thank Arlyn Andrews at NOAA/ESRL for the CO_2 concentration data at WBI, John Baker (USDA-ARS) and Tim Griffis (University of Minnesota) for the flux data at Rosemount, Roser Matamala from the Argonne National Laboratory for the data at the Fermi Agricultural site, and Shashi Verma at the University of Nebraska-Lincoln for the Mead flux data. The authors also thank Rachel Law (CSIRO) for all of her help and suggestions and Ying-Ping Wang (CSIRO) for constructive comments on the manuscript. Support for the writing of this work has been granted as part of the Australian Climate Change Science Program, funded jointly by the Department of Climate Change, the Bureau of Meteorology, and CSIRO. This research was funded by the National Oceanic and Atmospheric Administration (NOAA) contract NA08OAR4320893, the National Institute for Climate Change Research (NICCR) grant MTU 050516Z14 and the Department of Energy contract DE-FG02-06ER64317. The authors thank the constructive comments by two anonymous reviewers, which improved the quality of the paper.

References

Andrews, A. E., Kofler, J. D., Bakwin, P. S., Zhao, C. and Tans, P. 2009. Carbon dioxide and carbon monoxide dry air mole fractions from the NOAA ESRL tall tower network, 1992–2009. Version: 2009–05-12, ftp://ftp.cmdl.noaa.gov/ccg/towers/.

Baker, I. T. and Denning, A. S. 2008. SiB3 modeled global 1-degree hourly biosphere-atmosphere carbon flux, 1998–2006. In: *Data set*. Oak Ridge National Laboratory Distributed Active Archive Center, Oak Ridge, TN, USA, http://daac.ornl.gov/.

Baldocchi, D., Falge, E., Gu, L. H., Olson, R., Hollinger, D. and coauthors. 2001. FLUXNET: a new tool to study the temporal and spatial variability of ecosystem-scale carbon dioxide, water vapor, and energy flux densities. *B. Am. Meteor. Soc.* **82**, 2415–2434.

Betts, R. A. 2005. Integrated approaches to climate-crop modelling: needs and challenges. *Phil. Trans. R. Soc. B* **360**, 2049–2065, doi:10/1098/rstb.2005.1739.

Bonan, G. B. 1997. Effects of land use on the climate of the United States. *Climatic Change* **37**, 449–486.

Bondeau, A., Smith, P. C., Zaehle, S., Schaphoff, S., Lucht, W. and coauthors. 2007. Modelling the role of agriculture for the 20th century global terrestrial carbon balance. *Global Change Biol.* **13**, 679–706, doi:10.1111/j.1365-2486.2006.01305.x.

Copeland, J. H., Pielke, R. A. and Kittel, T. G. F. 1996. Potential climatic impacts of vegetation change: a regional modeling study. *J. Geophys. Res.-Atmos* **101**(D3), 7409–7418.

Corbin, K. D., Denning, A. S., Lu, L., Wang, J.-W. and Baker, I. T. 2008. Using a high resolution coupled ecosystem-atmosphere model to estimate representation errors in inversions of satellite CO_2 retrievals. *J. Geophys. Res.-Atmos* **113**(D02301), doi:10.1029/2007JD008716.

Crosson, E. R. 2008. A cavity ring-down analyzer for measuring atmospheric levels of methane, carbon dioxide, and water vapor. *Appl. Phys. B* **92**(3), 403–408.

Denning, A. S., Nicholls, M., Prihodko, L., Baker, I. T., Vidale, P.-L. and co-authors. 2003. Simulated variations in atmospheric CO_2 over a Wisconsin forest using a coupled ecosystem-atmosphere model. *Global Change Biol.* **9**, 1241–1250.

De Noblet-Ducoudre, N., Gervois, S., Ciais, P., Viovy, N., Brisson, N. and co-authors. 2004. Coupling the Soil-Vegetation-Atmosphere-Transfer Scheme ORCHIDEE to the agronomy model STICS to study the influence of croplands on the European carbon and water budgets. *Agronomie* **24**, 397–407, doi:10.1051/agro:2004038.

Energy Information Administration. 2007. Emissions of greenhouse gases. Report DOE/EIA-0573. Office of Integrated Analysis and Forecasting. U.S. Department of Energy, Washington, DC, 64.

Frietas, S. R., Longo, K. M., Silva Dias, M. A. F., Silva Dias, P. L., Chatfield, R. and co-authors. 2005. Monitoring the transport of biomass burning emissions in South America. *Environ. Fluid Mech.* **5**(1–2), 135–167.

Gervois, S., de Noblet-Ducoudre, N., Viovy, N. and Ciais, P. 2004. Including croplands in a global biosphere model: methodology and evaluation at specific sites. *Earth Interact.* **8**(16), 1–25.

Griffis, T. J., Sargent, S. D., Baker, J. M., Lee, X., Tanner, B. D. and co-authors. 2008. Direct measurement of biosphere-atmosphere isotopic CO_2 exchange using the eddy covariance technique. *J. Geophys. Res.-Atmos.* **113**(D08304), doi:10.1029/2007JD009297.

Gurney, K. R., Mendoza, D. L., Zhou, Y., Fischer, M. L., Miller, C. C. and co-authors. 2009. High resolution fossil fuel combustion CO_2 emission fluxes for the United States. *Environ. Sci. Technol.* **43**, doi:10.1021/es900806c.

Houghton, R. A. 2003. Revised estimates of the annual net flux of carbon to the atmosphere from changes in land use and land management 1850–2000. *Tellus* **55B**, 378–390.

International Geosphere Biosphere Programme (IGBP). 2000. Global soil data products CD-ROM (IGBP-DIS). In: *Global Soil Data Task*. Data and Information System, Potsdam, Germany. Available from Oak Ridge National Laboratory Distributive Active Archive Center, Oak Ridge, TN, USA, http://www.daac.ornl.gov.

Janssens, I. A., Freibauer, A., Ciais, P., Smith, P., Nabuurs, G.-J. and co-authors. 2003. Europe's terrestrial biosphere absorbs 7 to 12% of European anthropogenic CO_2 emissions. *Science* **300**(5625), 1538–1542.

Lawrence, D. M. and Slingo, J. M. 2004. An annual cycle of vegetation in a GCM. Part II: Global impacts on climate and hydrology. *Climate Dyn.* **22**, 107–122, doi:10.1007/s00382-003-0367-8.

Lokupitiya, E., Breidt, F. J., Lokupitiya, R., Williams, S. and Paustian, K. 2007. Deriving comprehensive county-level crop yield and area data for U.S. cropland. *Agron. J.*, **99**(3), 673–681.

Lokupitiya, E., Denning, A. S., Paustian, K., Baker, I. T., Schaefer, K. and co-authors. 2009. Incorporation of crop phenology in Simple Biosphere Model (SiBcrop) to improve land-atmosphere carbon exchanges from croplands. *Biogeosciences* **6**, 969–986.

Lu, L., Denning, A. S., da Silva-Dias, M. A., da Silva-Dias, P., Longo, M. and co-authors. 2005. Mesoscale circulations and atmospheric CO_2 variations in the Tapajos Region, Para, Brazil. *J. Geophys. Res.-Atmos.* **110**(D21102), doi:10.1029/2004JD005757.

Matamala, R., Jastrow, D. J., Miller, R. M. and Garten, C. 2008. Temporal changes in the distribution of C and N stocks in a restored tallgrass prairie in the U.S. Midwest. *Ecol. Appl.* **18**, 1470–1488.

Mesinger, F., DiMego, G., Kalnay, E., Mitchell, K., Shafran, P. C. and co-authors. 2006. North American Regional Reanalysis. *Bull. Am. Meteorol. Soc.* **87**(3), 343–360.

Nicholls, M. E., Denning, A. S., Prihodko, L., Vidale, P.-L., Baker, I. T. and co-authors. 2004. A multiple-scale simulation of variations in atmospheric carbon dioxide using a coupled biosphere-atmospheric model. *J. Geophys. Res.-Atmos.* **109**(D18117), doi:10.1029/2003JD004482.

Ogle, S., Davis, K. J., Andrews, A., Gurney, K. R., West, T. and co-authors. 2006. Mid-continent intensive campaign of the North America Carbon Program. *Sci. Plan.*, http://www.nacarbon.org/nacp/mci.html.

Osborne, T. M., Lawrence, D. M., Challinor, A. J., Slingo, J. M. and Wheeler, T. R. 2007. Development and assessment of a coupled crop-climate model. *Global Change Biol.* **13**, 169–183, doi:10.1111/j.1365-2486.2006.01274.x.

Parazoo, N. C., Denning, A. S., Kawa, S. R., Corbin, K. D., Lokupitiya, R. S. and co-authors. 2008. Mechanisms for synoptic variations of atmospheric CO_2 in North America, South America, and Europe. *Atmos. Chem. Phys.* **8**, 7239–7254.

Ramankutty, N. and Foley, J. A. 1998. Characterizing patterns of global land use: an analysis of global croplands data. *Global Biogeochem. Cycles* **12**(4), 667–685.

Richardson, S. J., Miles, N. L., Davis, K. J., Crosson, E., Van Pelt, A. D. and co-authors. 2009. *EOS Trans. AGU* **90**(52), Fall Meet. Suppl., Abstract B51E-0343.

Verma, S. B., Dobermann, A., Cassman, K. G., Walters, D. T., Knops, J. M. and co-authors. 2005. Annual carbon dioxide exchange in irrigated and rainfed maize-based agroecosystems. *Agric. Forest. Met.* **131**(1–2), 77–96.

Vleeshouwers, L. M. and Verhagen, A. 2002. Carbon emission and sequestration by agricultural land use: a model study for Europe. *Global Change Biol.* **8**, 519–530.

Wang, J.-W., Denning, A. S., Lu, L., Baker, I. T., Corbin, K. D. and co-authors. 2007. Observations and simulations of synoptic, regional, and local variations in atmospheric CO_2. *J. Geophys. Res.-Atmos.* **112**(D04108), doi:10.1029/2006JD007410.

Xiao, J. F., Zhuang, Q. L., Baldocchi, D. D., Law, B. E., Richardson, A. D. and co-authors. 2008. Estimation of net ecosystem carbon exchange for the conterminous United States by combining MODIS and AmeriFlux data. *Agric. Forest Met.* **148**(11), 1827–1847.

Zhao, M., Heinsch, F. A., Nemani, R. R. and Running, S. W. 2005. Improvements of the MODIS terrestrial gross and net primary production global data set. *Rem. Sens. Environ.* **95**, 164–176.